

UNIVERSITY OF BERGEN

A High-granularity Digital Tracking Calorimeter developed for proton CT

Viljar Nilsen Eikeland
on behalf of the Bergen pCT collaboration

UNIVERSITY OF BERGEN



Outline

- Proton Computed Tomography
- Mechanical Design of the Bergen pCT
- Results from various beam tests
- Image Reconstruction
- Outlook and other uses



Proton Computed Tomography

- Treatment with charged particles reduces dose delivery to healthy tissue
- Uncertainty of Bragg-peak placement when image is acquired with conventional CT
- Particle imaging allows for the direct measure of particle range within target

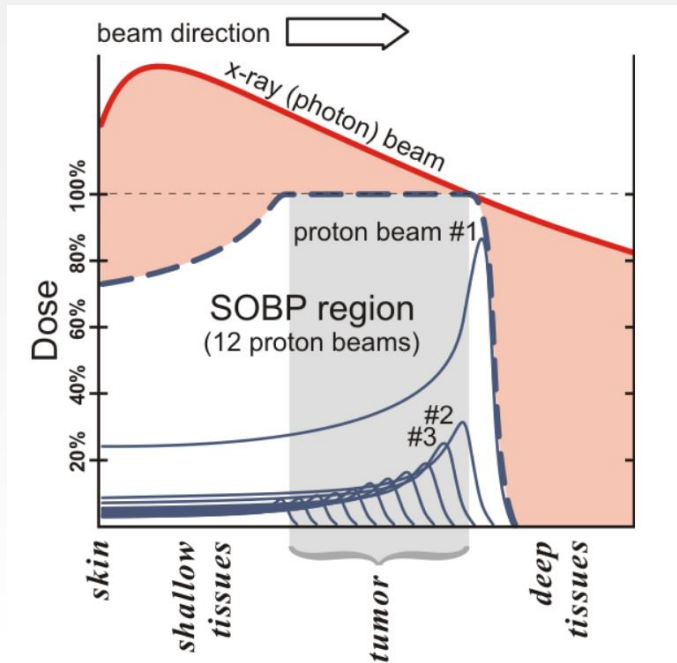


Figure 1: The different depth dose distributions from photons and protons, as a function of depth in water [1]

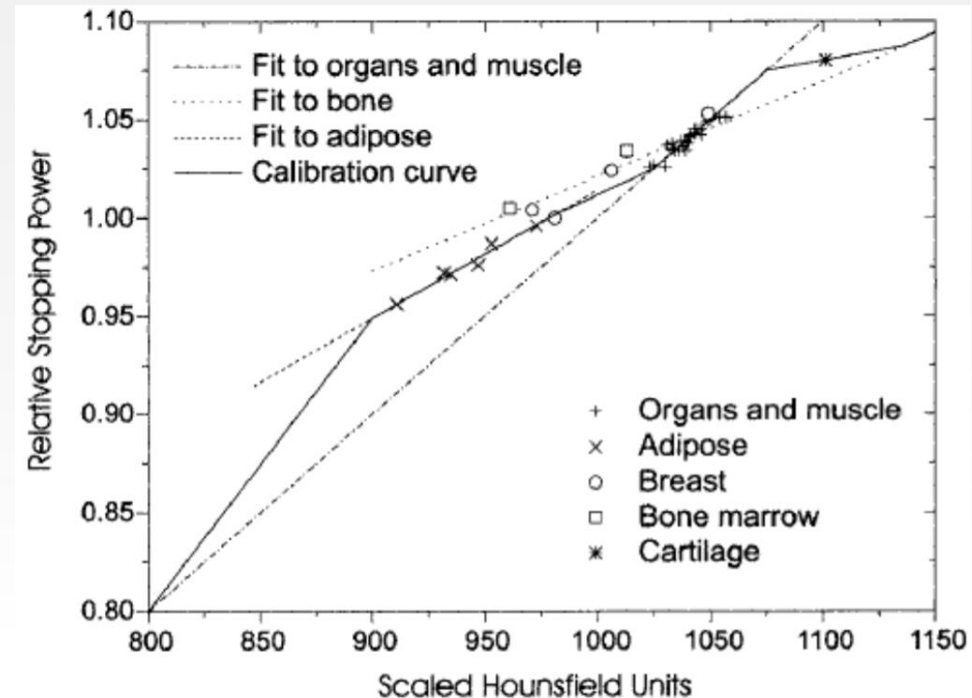


Figure 2: RSP as a function of HU [2]



Requirements and design choices

- Requirements:
 - Fast readout speed
 - High-granularity
- Single-sided Imaging setup
- Digital Tracking Calorimeter
 - Layer-by-layer
 - Silicon pixel sensors used as both tracking and energy detectors

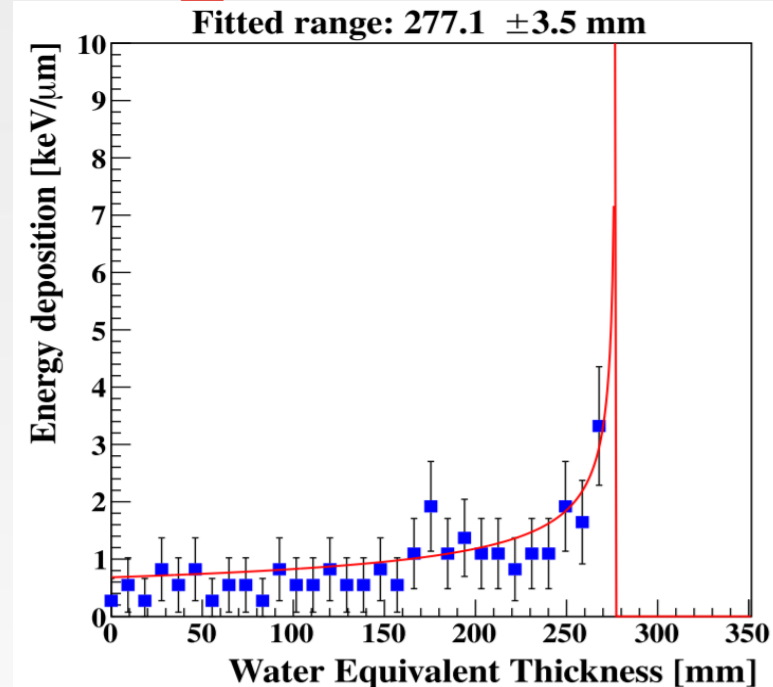
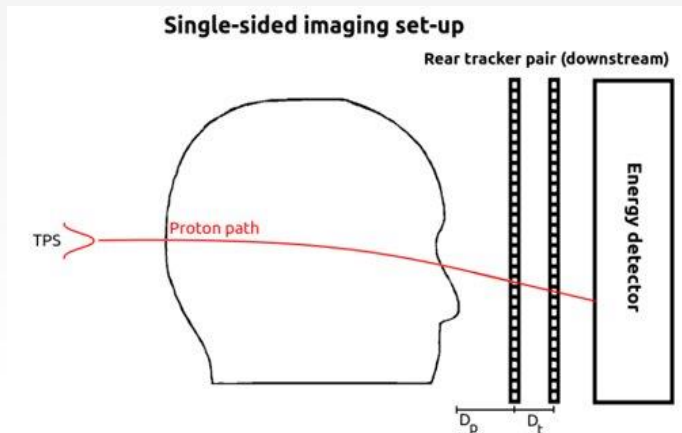
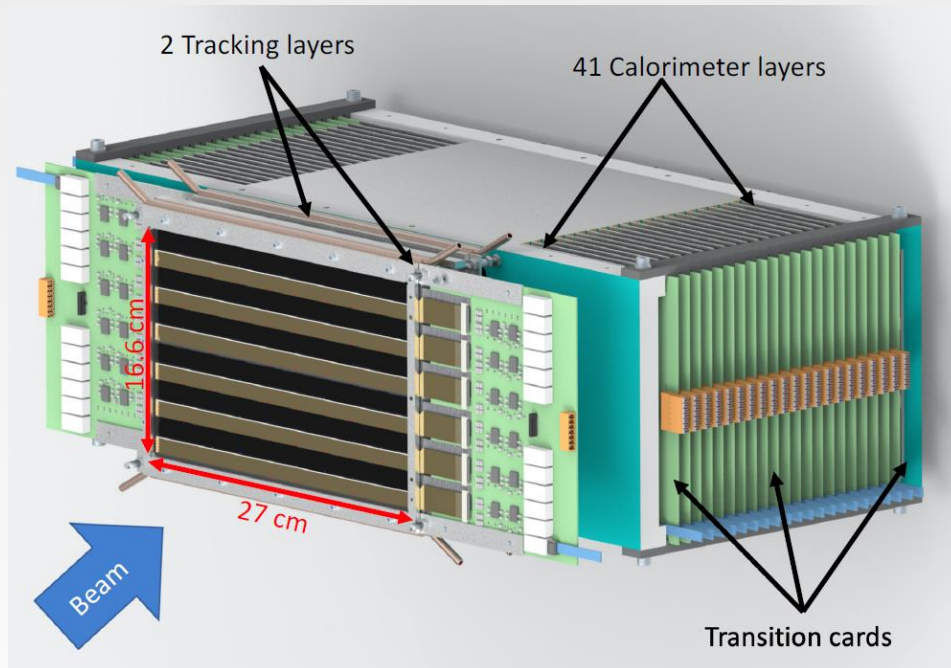


Figure 3 (bottom left): Single sided proton computed tomography [3]

Figure 4 (Top right): Energy deposition as a function of depth, fit by Bragg-Kleeman equation [4]



Digital Tracking Calorimeter

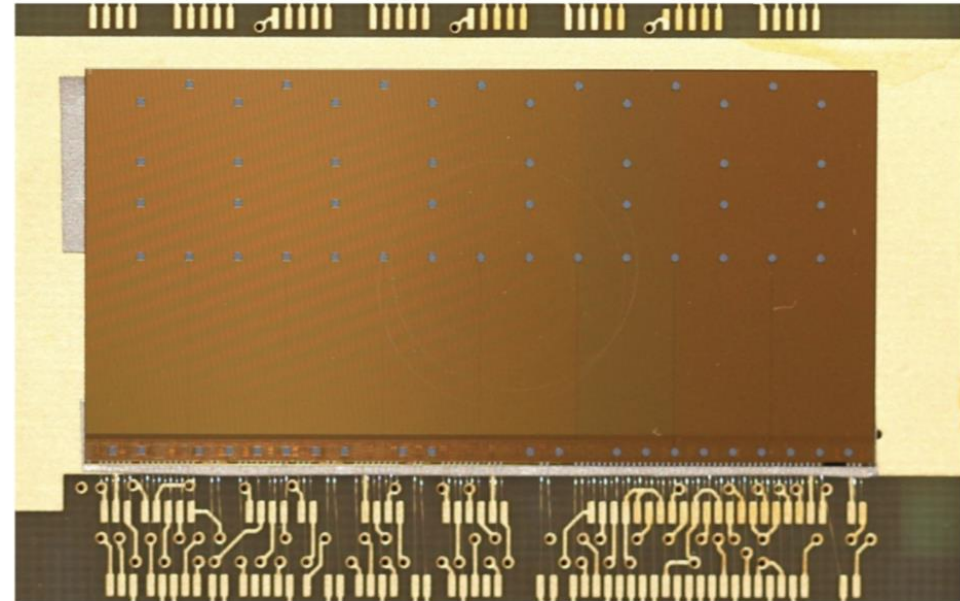


- 108 ALPIDEs on each layer
- Two tracking layers
 - 50 μm ALPIDE mounted on $\sim 300 \mu\text{m}$ carbon sheets
- 41 Calorimeter layers
 - 100 μm ALPIDE
 - 3 mm aluminium absorber

Figure 5: Schematic of the Bergen pCT detector [6]

ALPIDE sensor

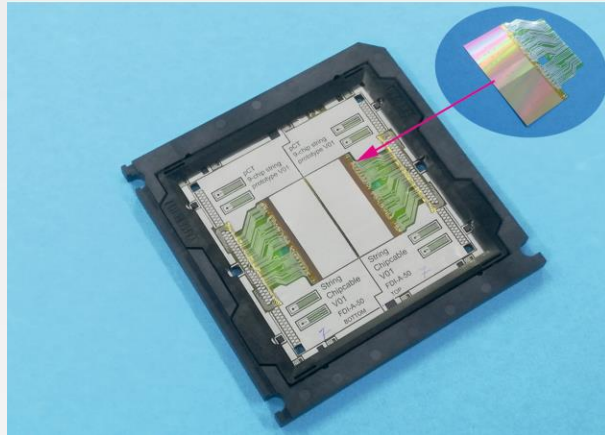
- Monolithic Active Pixel Sensor
- Pixel size: $29.24 \mu\text{m} \times 26.88 \mu\text{m}$
- Pixel matrix: 1024×512
- Peaking time $\sim 2\mu\text{s}$
- 3 in-pixel memories



- Figure 6: Photograph of the ALPIDE. Interface pads used for bonding to the printed circuit board are visible (gray squares). [6]

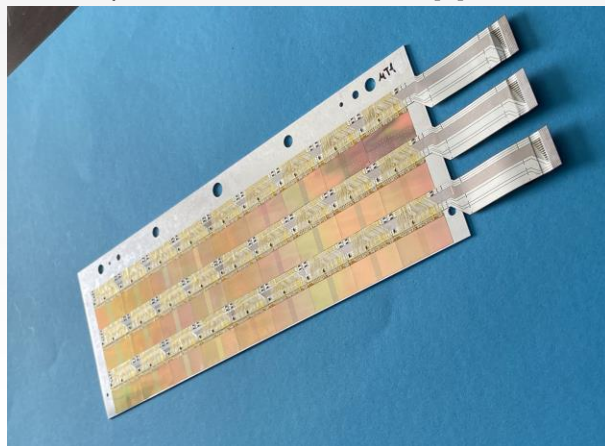


Mounting process of a layer

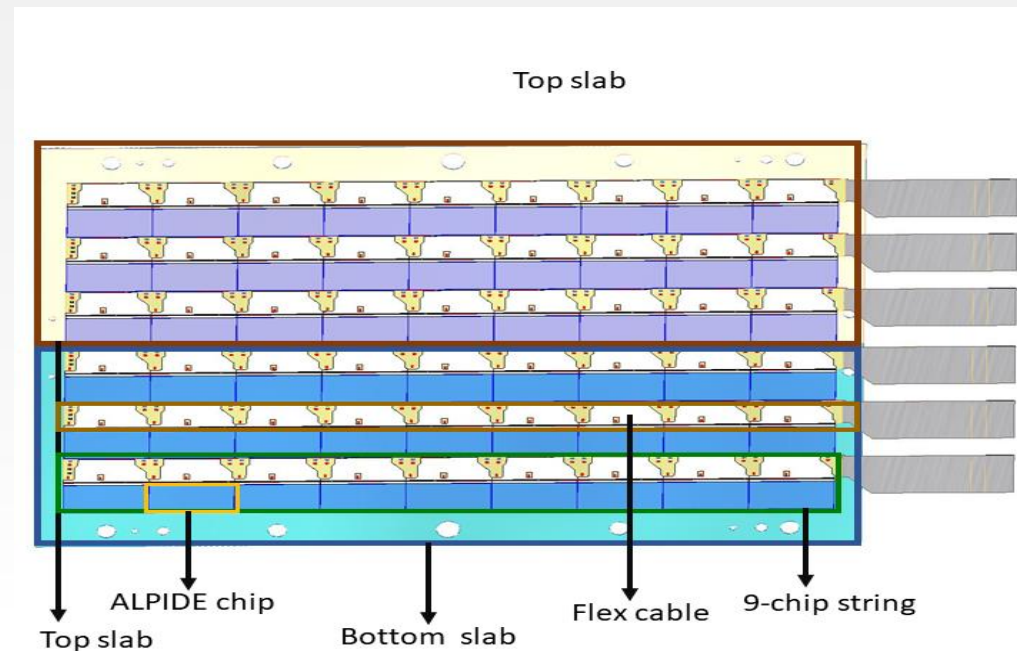


- Bonded to Chip Cable by Single-Point Tape Automated Bonding
- Nine sensors bonded on flex is known as a 9-chip string
- Three 9-chip strings constitutes a slab
- Two half layers face to face cover the full area

• Figure 7: Photograph of the ALPIDE chips bonded to a flex-cable [6]



• Figure 8: Photograph of the ALPIDE chips on slab



• Figure 9: Half a layer consists of ALPIDEs on aluminum carrier [6]

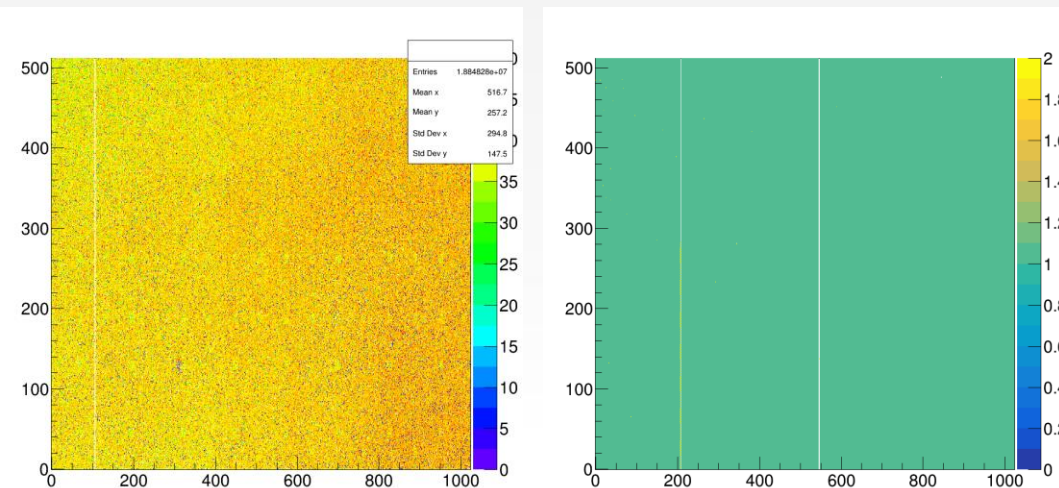


Verification during mounting process



• Figure 10: Photograph of the production test box used for verification of the ALPIDE sensors after bonding.

- ALPIDE is tested multiple times during the mounting process.
 - Power Test to look for shorts in the pixel-matrix
 - Digital scans to validate the communication with the sensor
 - Matrix scans to evaluate the response of the front-end electronics



• Figure 11: (left) Threshold scan (right) Analog scan



Tracking Layers

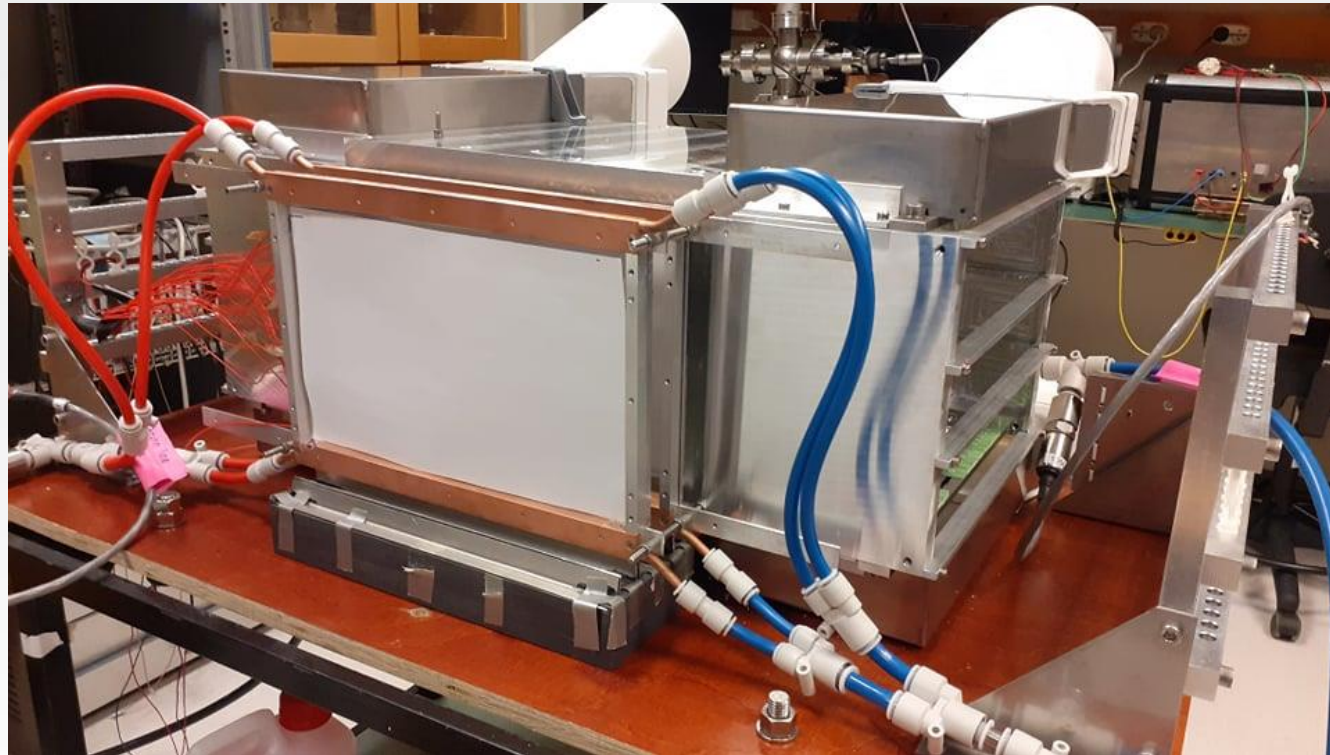


- Figure 12: Sandwiched Carbon Fiber sheet
200 mm x 290 mm x 0.3 mm

- Thinned ALPIDE sensors mounted on carbon sheet
 - Thickness 50 μm
- Carbon sheet with total thickness ~300 μm
- Carbon sheet is mounted in aluminium frame
- Materials used in carbon sheet:
 - Pyrolytic graphite paper
 - Carbon Fleece
 - Epoxy Resin



Mechanical Structure and Cooling



- Support structure for carbon sheets
- Water cooling of sensor layers
- Air cooling of transition cards

• Figure 13: Photograph of the mechanical structure



Readout

- Transition Card to act as intermediate between front-end and readout unit
- Custom readout unit based on Xilinx Kintex Ultrascale FPGA
- One readout unit per layer (108 ALPIDEs)
- Motherboard to synchronize triggering signal
- Can support up to four Independent 10 Gbit links

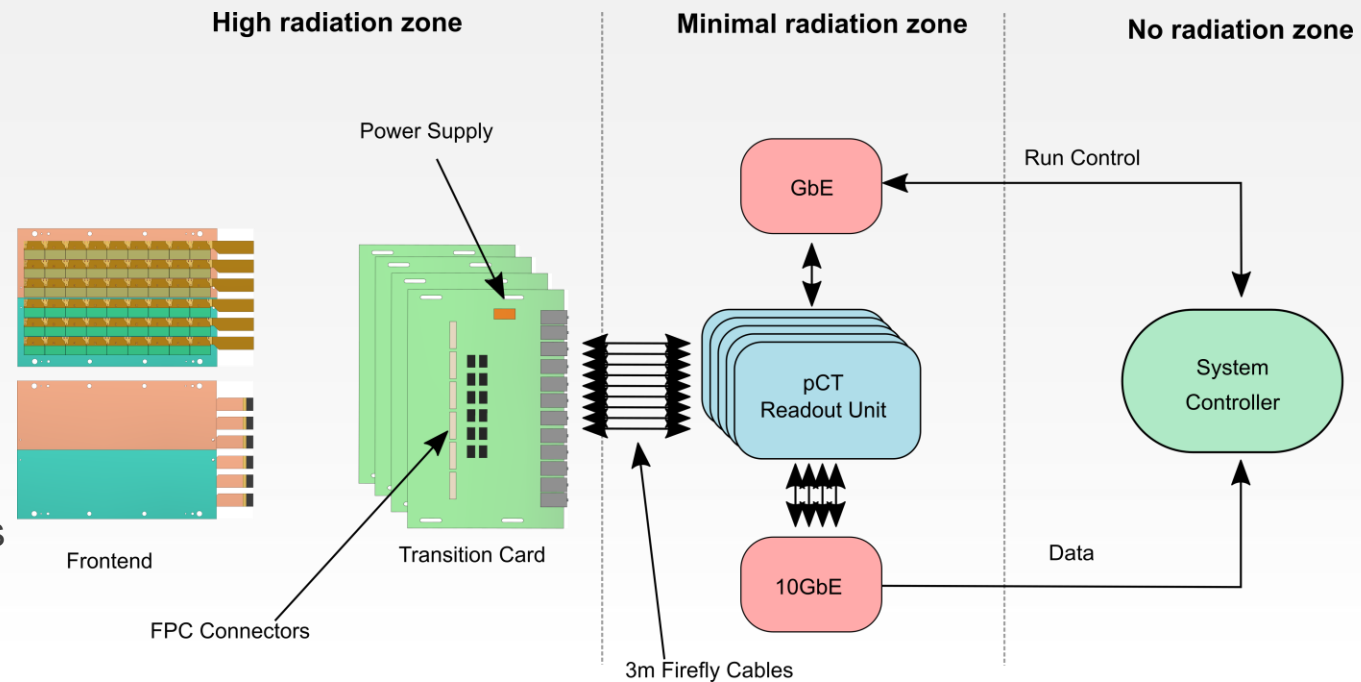


Figure 14: The pCT system electronics architecture. [6]



Energy deposition in ALPIDE

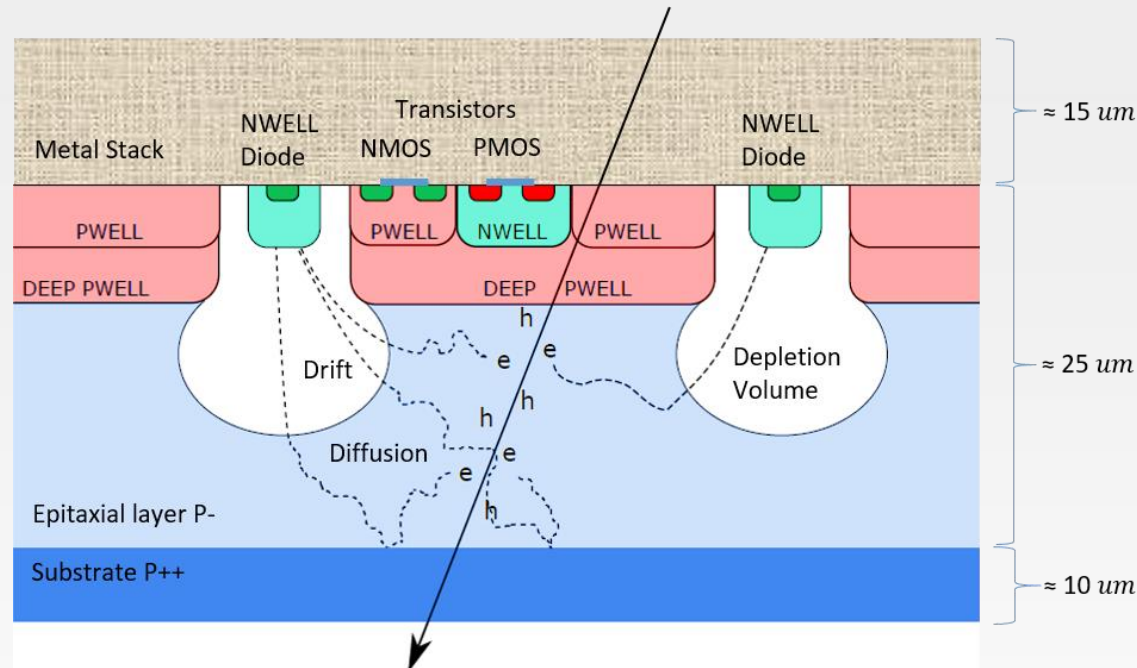


Figure 15: ALPIDE front-end [7]

- Incoming particle deposits energy in the epitaxial layer
- The signal may spread to multiple collection diodes
- Possibility of back-biasing the collection diodes up to $-6V$
 - $-3V$ to be applied in tracking layers

Energy measurements

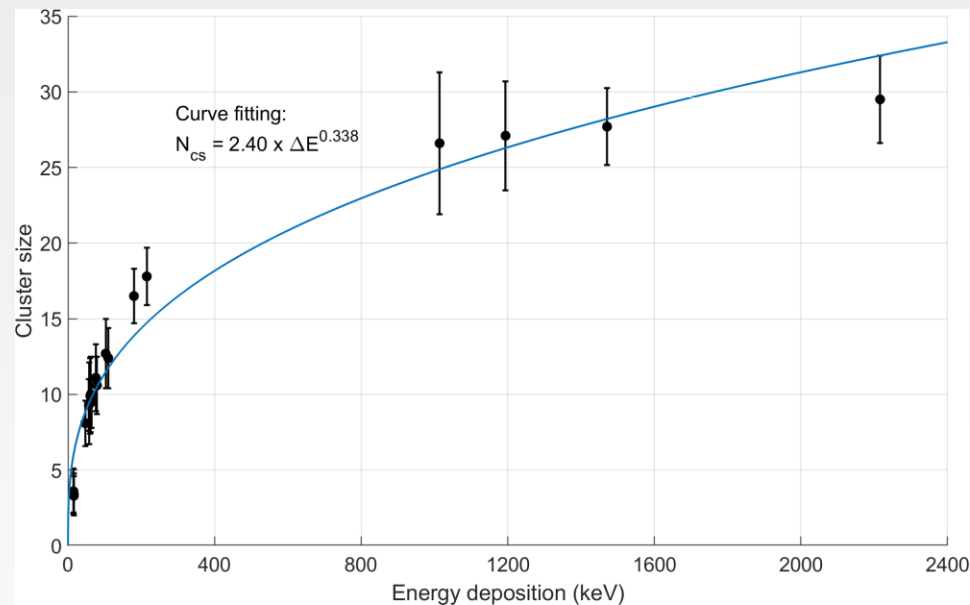


Figure 16: Measured Cluster Size vs energy deposition. [6]

- Correlation between cluster size and deposited energy
- Penetration depth in DTC will provide information about the initial energy of the particle

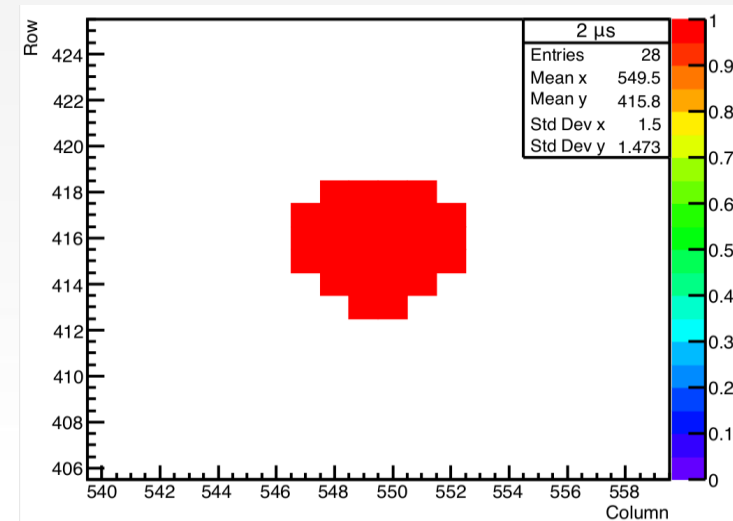


Figure 17: Single Cluster from an alpha source. [6]



Occupancy Studies

- Pencil beam to be used for pCT
 - ~3 mm beamspot
 - $\sim 10^6$ protons per beam spot
- ALPIDE
 - 3 in-pixel memories
 - 50 ns to read and clear pixel
 - Integration time $\sim 4\mu\text{s}$
- Busy Flag
 - Indicates that last available memory is used for writing current frame
- Busy Violation
 - No available memory for current frame
- Limiting factor is number of hits in region as hits are read out sequentially

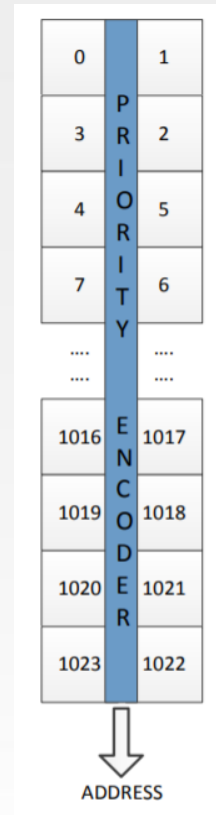


Figure 19: Priority Encoder [7]

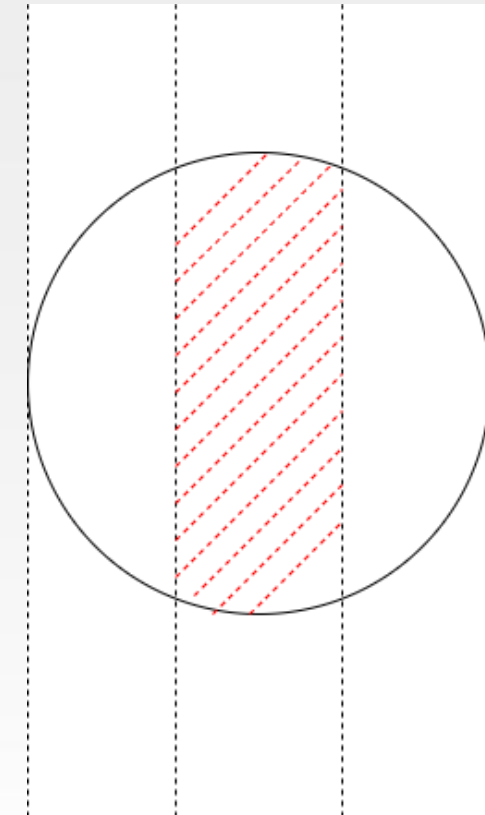


Figure 20: Pencil beam over ALPIDE region. Only illustrative purpose.



Occupancy studies

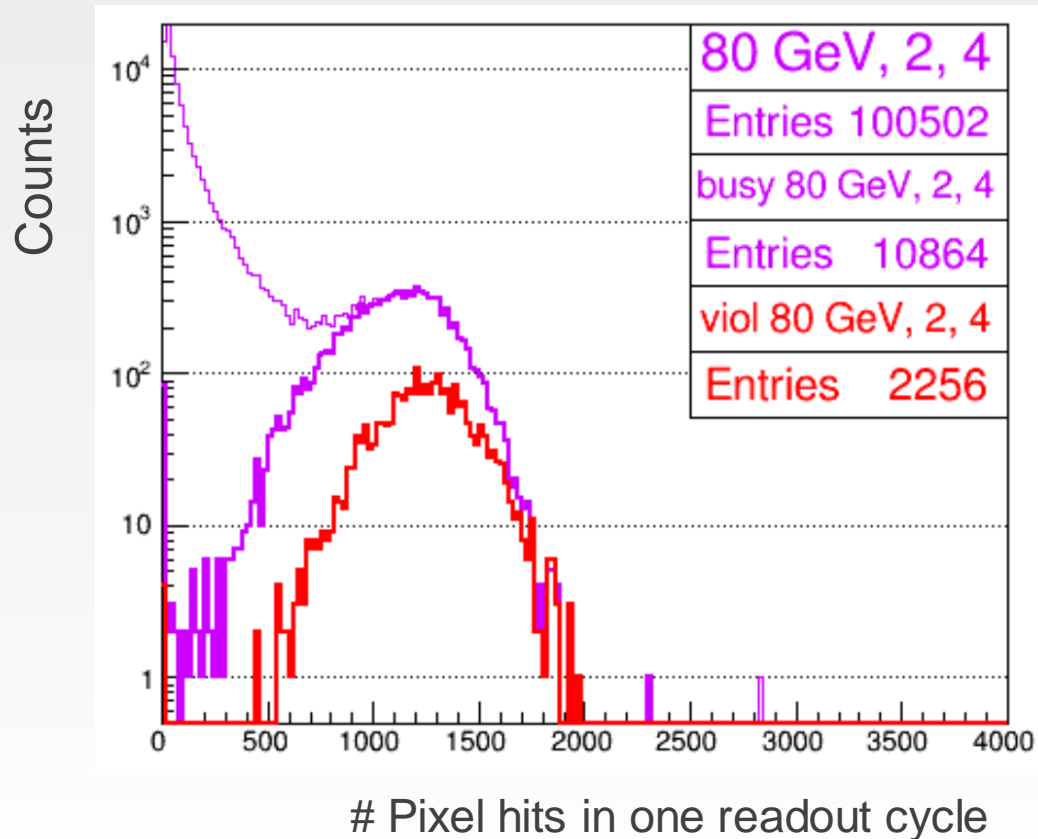


Figure 21: Busy Violations as a function of hits in ALPIDE

- ALPIDE placed in 80 GeV beam (mixed)
- ALPIDE placed behind 5 and 10 layers of tungsten
 - Thickness 3.5 mm
- Continuous trigger rate of 100 kHz, (same trigger system as in final DTC)
- ALPIDE should be able to handle a rate of $\sim 5 \cdot 10^6$ [protons/s] in pencil beam with 3 mm beamspot, assuming no scattering in patient/phantom

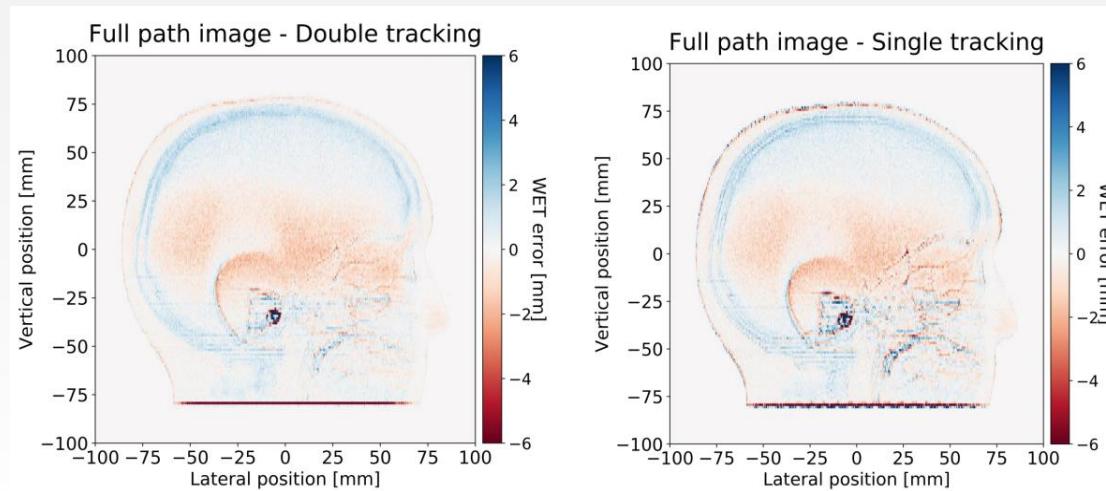
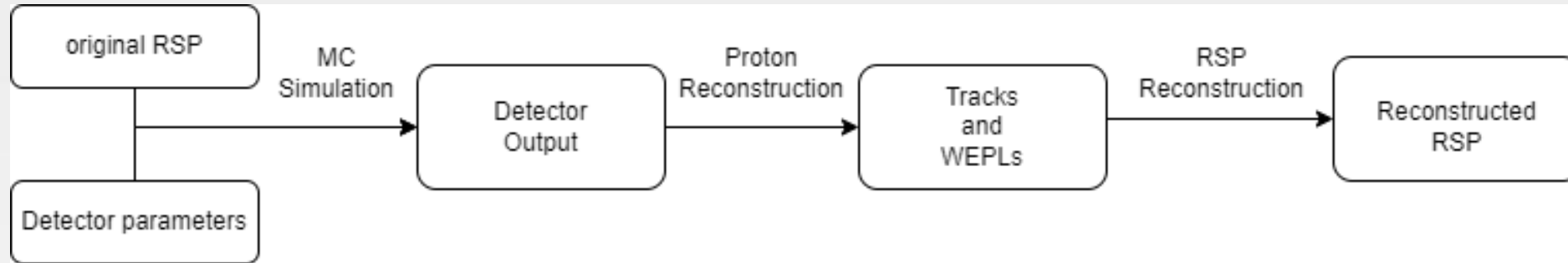


Image Reconstruction

- The energy of the incoming proton is estimated by a fit of the Bragg-Kleeman equation, and converted to water-equivalent path length (WEPL)
- Track reconstruction in DTC
- Most Likely Path (MPL) to estimate proton trajectory
- To reconstruct the relative stopping power (RSP) in the phantom/patient from the tracks and WEPLs, solve a linear system $A \cdot RSP = WEPL$. The matrix A depends on the tracks and geometry.



Reconstruction based on simulation



• Figure 22: WET errors for different tracking setups [8]

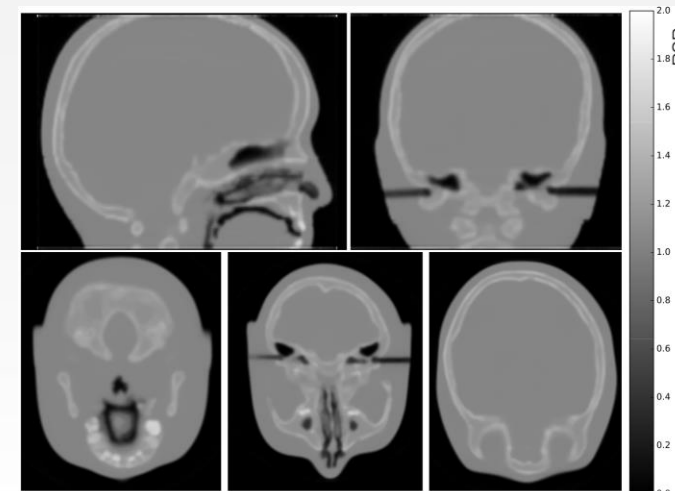


Figure 23: pCT reconstruction of the simulated head phantom in the modeled setup. [6]



Outlook and other uses

- Mechanical design is complete
- Mass production of sensor layers
- Expected to be installed in medical facilities in 2024
- Online applications during treatment





Thank you for your attention

Viljar.eikeland@uib.no

<https://www.frontiersin.org/articles/10.3389/fphy.2020.568243/full>

References

- [1] Filipak, M. (2012). Comparison of dose profiles for proton vs x-ray radiotherapy. <https://commons.wikimedia.org/w/index.php?curid=27983203>. CC BY-SA 3.0, Accessed: 2022-10-02. 2
- [2] B Schaffner and E Pedroni 1998 *Phys. Med. Biol.* 43 1579
- [3] Taheri-Kadkhoda, Z., Björk-Eriksson, T., Nill, S. *et al.* (2008) Intensity-modulated radiotherapy of nasopharyngeal carcinoma: a comparative treatment planning study of photons and protons
- [4] Helge Seime Pettersen, A Digital Tracking Calorimeter for Proton Computed Tomography, phd thesis
- [5] Jarle Rambo Sølve *et al* 2020 *Phys. Med. Biol.* 65 135012
- [6] Alme et al. A high granularity digital tracking calorimeter optimized for proton ct. *Frontiers in Physics*, 8:460, 2020.
- [7]ALICE ITS ALPIDE development team. Alpide operations manual.
- [8] Collins-Fekete, C.-A, et al., (2016). A Maximum likelihood method for high resolution proton radiography/proton CT, *Physics in medicine and Biology* 61 (23): 8232.

